Available online at www.sciencedirect.com

SciVerse ScienceDirect

Geochimica et Cosmochimica Acta 75 (2011) 6844–6858

Geochimica et Cosmochimica Acta

www.elsevier.com/locate/gca

Dependence of microbial magnetite formation on humic substance and ferrihydrite concentrations

Annette Piepenbrock, Urs Dippon, Katharina Porsch [1], Erwin Appel, Andreas Kappler *

Center for Applied Geosciences, Eberhard Karls University of Tuebingen, Sigwartstrasse 10, D-72076 Tuebingen, Germany

Received 15 February 2011; accepted in revised form 29 August 2011; available online 8 September 2011

Abstract

Iron mineral (trans)formation during microbial Fe(III) reduction is of environmental relevance as it can influence the fate of pollutants such as toxic metal ions or hydrocarbons. Magnetite is an important biomineralization product of microbial iron reduction and influences soil magnetic properties that are used for paleoclimate reconstruction and were suggested to assist in the localization of organic and inorganic pollutants. However, it is not well understood how different concentrations of Fe(III) minerals and humic substances (HS) affect magnetite formation during microbial Fe(III) reduction. We therefore used wet-chemical extractions, magnetic susceptibility measurements and X-ray diffraction analyses to determine systematically how (i) different initial ferrihydrite (FH) concentrations and (ii) different concentrations of HS (i.e. the presence of either only adsorbed HS or adsorbed and dissolved HS) affect magnetite formation during FH reduction by *Shewanella oneidensis* MR-1. In our experiments magnetite formation did not occur at FH concentrations lower than 5 mM, even though rapid iron reduction took place. At higher FH concentrations a minimum fraction of Fe(II) of 25–30% of the total iron present was necessary to initiate magnetite formation. The Fe(II) fraction at which magnetite formation started decreased with increasing FH concentration, which might be due to aggregation of the FH particles reducing the FH surface area at higher FH concentrations. HS concentrations of 215–393 mg HS/g FH slowed down (at partial FH surface coverage with sorbed HS) or even completely inhibited (at complete FH surface coverage with sorbed HS) magnetite formation due to blocking of surface sites by adsorbed HS. These results indicate the requirement of Fe(II) adsorption to, and subsequent interaction with, the FH surface for the transformation of FH into magnetite. Additionally, we found that the microbially formed magnetite was further reduced by strain MR-1 leading to the formation of either dissolved Fe(II), i.e. Fe^{2+}, in HEPES buffered medium or Fe(II) carbonate (siderite) in bicarbonate buffered medium. Besides the different identity of the Fe(II) compound formed at the end of Fe(III) reduction, there was no difference in the maximum rate and extent of microbial iron reduction and magnetite formation during FH reduction in the two buffer systems used. Our findings indicate that microbial magnetite formation during iron reduction depends on the geochemical conditions and can be of minor importance at low FH concentrations or be inhibited by adsorption of HS to the FH surface. Such scenarios could occur in soils with low iron mineral or high organic matter content.

* Corresponding author. Tel.: +49 7071 2974992; mobile: +49 172 7263202; fax: +49 7071 295059.
E-mail address: andreas.kappler@uni-tuebingen.de (A. Kappler).
[1] Present address: Helmholtz Centre for Environmental Research – UFZ, Department of Bioenergy, Permoserstrasse 15, D-04318 Leipzig, Germany.

0016-7037/$ - see front matter © 2011 Elsevier Ltd. All rights reserved.
doi:10.1016/j.gca.2011.09.007

1. INTRODUCTION

Iron is ubiquitous in almost all aquatic and terrestrial environments and is present at neutral pH mostly in the form of ferric and ferrous iron minerals such as goethite (α-FeOOH), hematite (α-Fe_2O_3), maghemite (γ-Fe_2O_3), poorly crystalline ferrihydrite (FH) (approx. $Fe(OH)_3$), magnetite (Fe_3O_4) and siderite ($FeCO_3$) (Cornell and Schwertmann, 2003). Under anoxic and low bicarbonate/low phosphate conditions, Fe(II) can also be present as dissolved Fe(II), i.e. Fe^{2+}, whereas the solubility of Fe(III) at neutral pH is very low in the absence of Fe(III)-chelating ligands. Iron readily undergoes redox reactions, which can be mediated either chemically or by Fe(II)-oxidizing and Fe(III)-reducing microorganisms (Kappler and Straub, 2005). Microbial iron reduction at neutral pH leads to the dissolution of Fe(III) minerals and to the formation of either dissolved Fe(II) or secondary mineral phases. The biomineralization products of dissimilatory Fe(III) reduction (e.g. magnetite, siderite, green rust) vary significantly depending on the geochemical conditions such as pH (Bell et al., 1987), buffer system (Fredrickson et al., 1998), reactivity of the Fe(III) minerals (Hansel et al., 2004), surface area of the Fe(III) minerals (Roden and Zachara, 1996), Fe(III) reduction rate (Zachara et al., 2002), electron donor:acceptor ratio (Fredrickson et al., 2003), cell concentration (O'Loughlin et al., 2010) and Fe(II) concentration (Hansel et al., 2005). Iron mineral (trans)formation affects the degradation, mobilization and immobilization of organic and inorganic pollutants and thus is of environmental relevance. For example, the degradation of organic pollutants can be coupled to Fe(III) mineral reduction (Lovley and Anderson, 2000). Additionally, toxic metal ions such as arsenic are removed from (Tufano and Fendorf, 2008) or released into (Islam et al., 2004) the environment during the formation and dissolution of iron minerals due to the sorption and co-precipitation of these metal ions to and into the iron mineral (Hohmann et al., 2010).

One of the most important mineral products of microbial Fe(III) reduction is the mixed-valent iron mineral magnetite (Hansel et al., 2005; Bazylinski et al., 2007). This ferrimagnetic iron mineral is an important iron ore and one of the most important factors determining magnetic soil properties. Thus, magnetite is of great paleogeo- and biological importance for paleoclimate reconstructions (Maher, 2009), the study of processes like the evolution of life on early earth (Cornell and Schwertmann, 2003; Johnson et al., 2003) and the deposition of iron deposits such as banded iron formations (BIFs). Microbial magnetite formation occurs either biologically controlled, i.e. in magnetotactic bacteria that use the magnetic properties of magnetite for orientation in the earth's magnetic field, or as a byproduct of microbial dissimilatory Fe(III) reduction and Fe(II) oxidation (Bazylinski et al., 2007). As changes in microbial magnetite formation might by perceptible as changes of the magnetic bulk signal, measurements of magnetic properties might be used to detect changes in microbial activity due to environmental contamination by organic pollution (Porsch et al., 2010). In order to apply magnetic measurements for the reliable localization of organic pollution, it is essential to understand the geochemical parameters controlling magnetite formation in the field. However, many lab studies use artificial systems with high concentrations of Fe(III) minerals and without environmentally relevant compounds such as humic substances (HS) present. It is currently unknown how different Fe(III) mineral concentrations and the presence of HS influence magnetite formation.

HS are known to be able to shuttle electrons between microorganisms and Fe(III) minerals thus enabling the microorganisms to overcome the limitation that is imposed on microbial Fe(III) reduction at neutral pH by the low solubility of the electron accepting Fe(III) minerals (see reviews by Kappler and Straub, 2005; Weber et al., 2006) (Fig. 1). Fe(III)-reducing bacteria have to get close to the Fe(III) minerals and transfer electrons either directly via outer-membrane proteins (Myers and Nealson, 1988) or, as recently shown, via conductive pili (Reguera et al., 2005; El-Naggar et al., 2010). Alternatively, Fe(III)-reducers can overcome the problem of the poor solubility of the Fe(III) minerals by using either iron chelators (Lovley et al., 1994) or electron shuttling compounds such as HS (Lovley et al., 1996) or flavins (Marsili et al., 2008; Von Canstein et al., 2008). HS are a heterogeneous mixture of polymeric organic molecules originating from the degradation of organic matter (Stevenson, 1994). They are ubiquitous in the environment, redox-active and they can be reduced not only by Fe(III)-reducing bacteria, but also by methanogens, sulfate-reducers (Cervantes et al., 2002) and fermenters (Benz et al., 1998). It was recently shown that Fe(III) reduction by *Shewanella oneidensis* MR-1 was stimulated by HS concentrations as low as 5–10 mg C/L and that Fe(III) reduction by *Geobacter sulfurreducens* via electron shuttling HS proceeded seven times faster than direct Fe(III) reduction (Jiang and Kappler, 2008). Both dissolved and solid-phase HS have been studied extensively with respect to their effect on microbial Fe(III) reduction due to electron shuttling (e.g. Lovley et al., 1996; Jiang and Kappler, 2008; Bauer and Kappler, 2009; Roden et al., 2010). Recently it has been suggested that HS also have an effect on the biomineralization products of microbial Fe(III) reduction, e.g. magnetite (Porsch et al., 2010). However, this effect has not been studied systematically so far.

As the structure of HS varies depending on genesis and isolation procedure, and due to their tendency to aggregate and precipitate under certain geochemical conditions and to sorb to minerals, HS are difficult to work with experimentally. Therefore, many researchers replaced HS in their studies on microbial Fe(III) reduction by simple model compounds for quinoid moieties in HS such as anthraquinone-2,6-disulfonic acid (AQDS) (e.g. Coates et al., 1998; Fredrickson et al., 1998). However, model quinones only model one of the functions of HS in microbial Fe(III) reduction systems (i.e. electron shuttling), and do not model other HS functions like sorption to iron minerals. Wolf et al. (2009) showed that sorption of HS to FH was more than one order of magnitude stronger than sorption of AQDS to FH. The effect of HS sorption on microbial iron reduction and magnetite formation has not yet been studied in detail. We hypothesize that HS influence magnetite

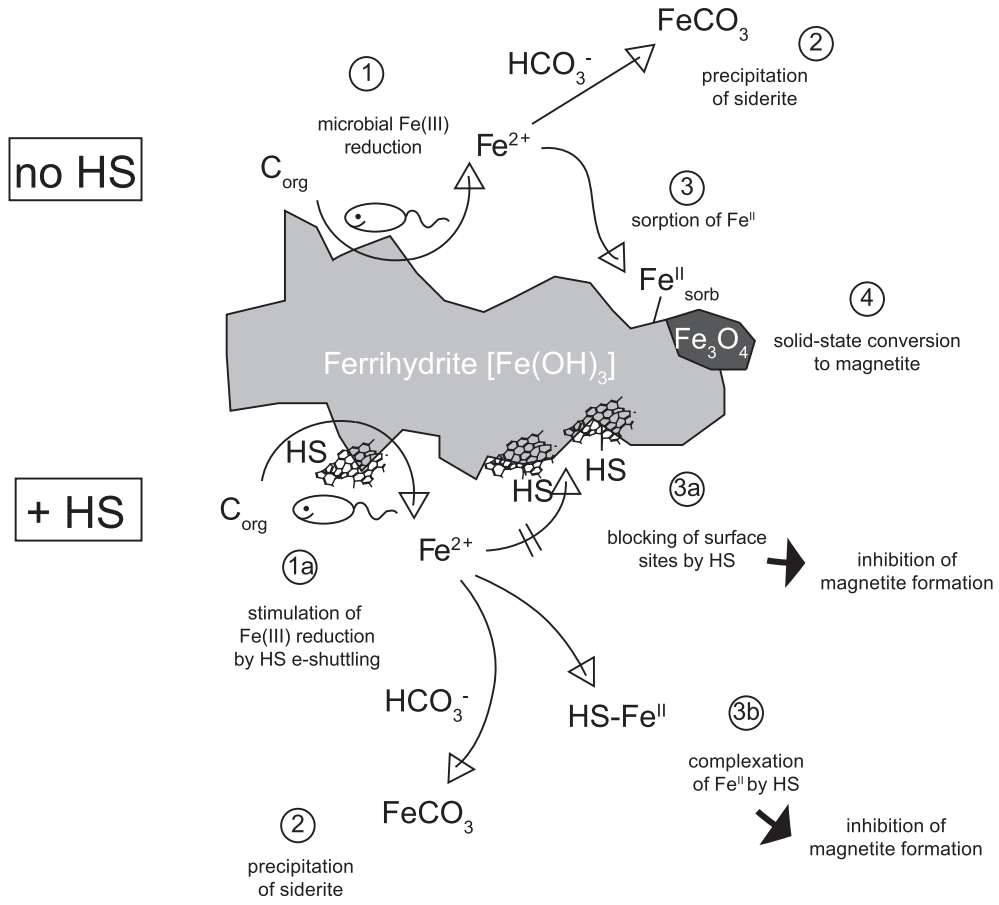

Fig. 1. Schematic illustration of the potential pathways of Fe(II) formed during microbial ferrihydrite (FH) reduction in the presence (lower part) and absence (upper part) of humic substances (HS). (1) Microbial reduction of FH produces Fe^{2+}, in the presence of HS this process can be stimulated (accelerated) by HS functioning as electron shuttles (1a). (2) Fe^{2+} interacts with bicarbonate (HCO_3^-) leading to the precipitation of siderite ($FeCO_3$). (3) Alternatively, Fe^{2+} sorbs to the FH surface, where the interaction of the sorbed Fe(II) (Fe^{II}_{sorb}) with the FH can lead to the solid-state conversion of FH to magnetite (Fe_3O_4) (4). In the presence of HS, Fe(II) sorption sites on the FH surface are blocked by sorbed HS (3a) inhibiting the solid-state conversion to magnetite. (3b) Additionally, the formation of complexes of HS with the Fe(II) (HS–Fe^{II}) reduces the amount of Fe(II) available for sorption to the FH surface and thus also inhibits solid-state conversion to magnetite.

formation by sorption to the ferrihydrite, by Fe(II) complexation and by changing the ferrihydrite reduction rates (Fig. 1). Therefore, this study aimed to determine the effect of (i) different initial FH concentrations and (ii) different concentrations of HS (i.e. the presence of either only sorbed HS or sorbed as well as dissolved HS) on iron mineral transformation, in particular on magnetite formation, during microbial FH reduction.

2. MATERIAL AND METHODS

2.1. Bacterial cultures and experimental set-up

S. oneidensis strain MR-1, originally isolated from Oneida Lake, New York (Myers and Nealson, 1988), was streaked out oxically from a frozen stock kept at −80 °C on Luria–Bertani (LB-medium) agar plates. LB-medium contained per L: 10 g tryptone, 5 g yeast extract, 5 g NaCl and 12 g agar. LB-plates were incubated at 28 °C for approximately 24 h and afterwards kept at 4 °C for up to 10 days. One colony was transferred into 10 mL of anoxic freshwater medium (Hegler et al., 2008) containing 20 mM lactate and 40 mM fumarate in a 23 mL culture tube. After 72 h of incubation at 28 °C in the dark, 200 µL were transferred into a fresh culture tube with freshwater medium. After another 24 h of incubation at 28 °C in the dark, cell concentration in the culture was determined by optical density (OD) measurements at 660 nm. OD_{660} was calibrated against cell counts obtained by direct counting with a Thoma-chamber by light microscopy (Axioscope 2, Zeiss, Germany). Dilutions of 2×10^7 cells/mL of these cultures were used as inocula for FH reduction experiments.

FH reduction experiments were conducted in LML medium (Myers and Myers, 1994), containing 20 mM lactate as electron donor and either 12 mM HEPES buffer or 30 mM bicarbonate buffer, adjusted to pH 7 and prepared aseptically and anoxically using a Widdel flask. Twenty five milliliter of anoxic LML medium were filled into sterile 50 mL serum bottles and the headspace was exchanged with N_2 for the HEPES buffered medium and N_2:CO_2 (90:10) for the bicarbonate buffered medium. FH, HS and AQDS solutions (for preparation see below) were added with a syringe

through the butyl rubber stopper to obtain final concentrations of 2.5–30 mM FH, 131–393 mg HS/g FH and 7.5–23.4 μM AQDS. The FH concentration was calculated using the simplified formula $Fe(OH)_3$. After 48 h on a horizontal shaker (200 rpm; IKA Labortechnik, Staufen, Germany) to allow equilibration of HS sorption to FH, the bottles were inoculated with 250 μL of the 2×10^7 cells/mL suspension (see above), yielding a final cell concentration of 2×10^5 cells/mL, and incubated at 28 °C in the dark.

HS sorption to FH was quantified under anoxic conditions in 30 mM bicarbonate buffered LML medium (see above) containing 20 mM lactate. Different concentrations of HS (100–700 mg/L) were added with a syringe through the stopper. The HS concentration was quantified before addition of 15 mM FH. After FH addition, the bottles were incubated for 72 h on a horizontal shaker (200 rpm; IKA Labortechnik, Staufen, Germany), centrifuged (10 min, 2000 rpm) and the HS concentration was quantified in the filtered (cellulose acetate, 0.2 μm, Fisher Scientific, Germany) supernatant.

2.2. Preparation of ferrihydrite suspensions, humic substance and AQDS solutions

FH was synthesized according to Schwertmann and Cornell (2000) and Raven et al. (1998) using 40 g of $Fe(NO_3)_3 \cdot 9H_2O$ per 500 mL water that was neutralized with 1 M KOH to a final pH of 7.2. After centrifugation and four washing steps with Millipore®-water, the wet solid was resuspended in water to an approximate concentration of 0.5 M Fe(III). The FH suspension was deoxygenized under vigorous stirring by alternating application of vacuum and N_2 for 3 min each and then stored in the dark at 4 °C. The iron concentration in the suspension was determined by the ferrozine assay. The FH was sterilized by autoclaving (121 °C, 1 bar overpressure, 20 min) and used within 6 weeks after synthesis for experiments.

For experiments with HS, IHSS (International Humic Substances Society) Pahokee Peat Humic Acid 1R103H2 was added to 88.6 mM NaCl solution at a concentration of either 5 or 10 g/L. The pH of the HS preparation was adjusted to 7.0 with NaOH. The HS preparation was filter-sterilized (cellulose acetate, 0.2 μm, Fisher Scientific, Germany) into autoclaved culture tubes closed with butyl rubber stoppers. After filtration, the solution was deoxygenated under sterile conditions by alternating application of vacuum and N_2 for 3 min each.

An AQDS stock solution of 1.25 mM was prepared by dissolution of 9,10-anthraquinone-2,6-disulfonic acid disodium salt in anoxic Millipore® water. After exchanging the headspace with N_2, the bottle was closed with a butyl rubber stopper and autoclaved (121 °C, 1 bar overpressure, 20 min).

2.3. Sampling and analytical methods

For quantitation of bioavailable Fe(tot) and Fe(II) concentrations, 100 μL samples were taken from the culture bottles with syringes and extracted with 900 μL of 0.5 M HCl for 2 h. Although samples were shaken thoroughly for homogenization, slight variation in amounts of precipitates in the samples taken could not be fully avoided. Visual observation of the samples showed that in some cases the 0.5 M HCl extraction method did not completely dissolve all minerals present. However, it has to be noted that the goal was not to quantify complete Fe(II) but bioavailable Fe(II). Fe(II) and Fe(tot) in the extracts were quantified using the ferrozine assay (Stookey, 1970) as described by Hegler et al. (2008). The detection limit of the ferrozine assay is in the low μM range. However, in this study the ferrozine assay was calibrated for a range of 10–1000 μM Fe.

Magnetite formation was followed by magnetic susceptibility (MS) measurements of the culture bottles. MS was measured using a KLY-3 Kappabridge (AGICO, Czech Republic) with a magnetic field intensity of 300 A/m and a frequency of 875 Hz at room temperature as described in Porsch et al. (2010). This study showed that MS monitoring is a suitable tool to follow microbial Fe mineral transformation non-invasively in batch cultures.

Maximum rates of microbial iron reduction and magnetite formation for the individual set-ups were calculated from the steepest slope between two subsequent measuring points of both the Fe(II) content and the MS measurements, and values were averaged between duplicates.

The sampling time points for μ-XRD were chosen individually for each experimental set-up depending on the MS values: one sample was taken immediately after inoculation ("start"), one during ("increase") one after the increase in MS ("plateau") and one sample at the end of the experiment ("end"). For each time point one bottle was harvested completely in order to obtain enough mineral product for μ-XRD and the complete mineral preparation was performed in an anoxic glove box (Braun, Germany; 100% N_2 atmosphere). The culture bottles were centrifuged (15 min, 2000 rpm), transferred into the glove box and the supernatant was discarded. The pellet was resuspended in anoxic Millipore® water and transferred into 2 mL plastic tubes. After washing three times with anoxic Millipore® water, the minerals were dried. The solids were grinded in an agate mortar and transferred to a silicon wafer. This was done in the anoxic glove box by suspending the mineral powder in anoxic ethanol, transferring it with a glass pipette or spatula, drying the minerals on the silicon wafer and then covering of the wafer with a low-density polyethylene foil to keep it anoxic during the measurement. Alternatively, the dry powder was transferred out of the glove box in an airtight glass jar and transferred onto the wafer (under air atmosphere) immediately before the measurement. This second preparation method involved a short exposure of the sample to air-oxygen. However, it was shown that exposure of chemically synthesized siderite to oxygen for several hours did not lead to any μ-XRD signals other than those of the siderite, even though the color of the mineral surface changed (Amstaetter, 2009). Furthermore, this preparation method had the advantage that the measurements could be done without the polyethylene foil, which otherwise caused a broad signal in the XRD-diffractogram in a 2θ range from 17° to 29°. In this range and at smaller angels the intensity of the X-rays diffracted by the mineral lattice

is reduced due to the foil. The μ-XRD-device (Bruker D8 Discover X-ray diffraction instrument, Bruker AXS GmbH, Germany) was set up using a Co K_α X-ray tube, operating at 30 kV, 30 mA. The EVA® 10.0.1.0 software was used to merge the three measured frames of one sample and to identify the containing mineral phases using the PDF-database licensed by ICDD (International Centre for Diffraction Data). The detection limit of the μ-XRD measurements was approximately 5% of the total iron mineral content. For details of μ-XRD analysis see Amstaetter et al. (2010).

HS concentrations were quantified by UV absorption at 465 nm using a quartz glass microtiter plate and a microtiter plate reader (FlashScan 550, Analytik Jena, Germany). A calibration curve was obtained in the range of 0–250 mg/L with a detection limit of 5 mg/L.

3. RESULTS AND DISCUSSION

3.1. Magnetite formation and transformation during ferrihydrite reduction: influence of media composition and ferrihydrite concentration

3.1.1. Medium and buffer system

In order to determine the effect of different geochemical conditions on magnetite formation, FH reduction experiments were set up with the Fe(III)-reducing bacterium *S. oneidensis* MR-1 in bicarbonate and HEPES buffered LML medium. The extent and maximum rates of Fe(III) reduction in 30 mM bicarbonate versus 12 mM HEPES buffered LML medium with 2.5–30 mM FH were very similar (Fig. 2). In these buffer systems up to 90.6 ± 1.6% and 85.5 ± 2.0% (for HEPES and bicarbonate buffered medium, respectively) of the Fe(III) was reduced and maximum reduction rates increased linearly with increasing FH concentration up to 15 mM FH (Fig. 2c and d). Similarly, no distinct differences in the change of the MS over time could be observed between bicarbonate and HEPES buffered LML medium (Fig. 3). For both buffer systems the MS increased rapidly in set-ups with ⩾5 mM FH during the first 5 days of incubation and then leveled off while in the set-ups with 2.5 mM FH no increase in MS was observed in both buffer systems. Magnetite was identified by μ-XRD measurements as the ferrimagnetic mineral phase responsible for the MS increase in bicarbonate buffered LML medium with 15 mM FH (Fig. 4) and in HEPES buffered LML medium with 5 and 10 mM FH (Fig. 5).

Magnetite formation during microbial Fe(III) reduction has frequently been described in cultures containing either bicarbonate buffer or PIPES buffer, another organic buffer structurally similar to HEPES (Zachara et al., 2002; Behrends and Van Cappellen, 2007; Bazylinski et al., 2007). Fredrickson et al. (1998) compared biomineral formation during FH reduction by *Shewanella putrefaciens* CN32 under different geochemical conditions including

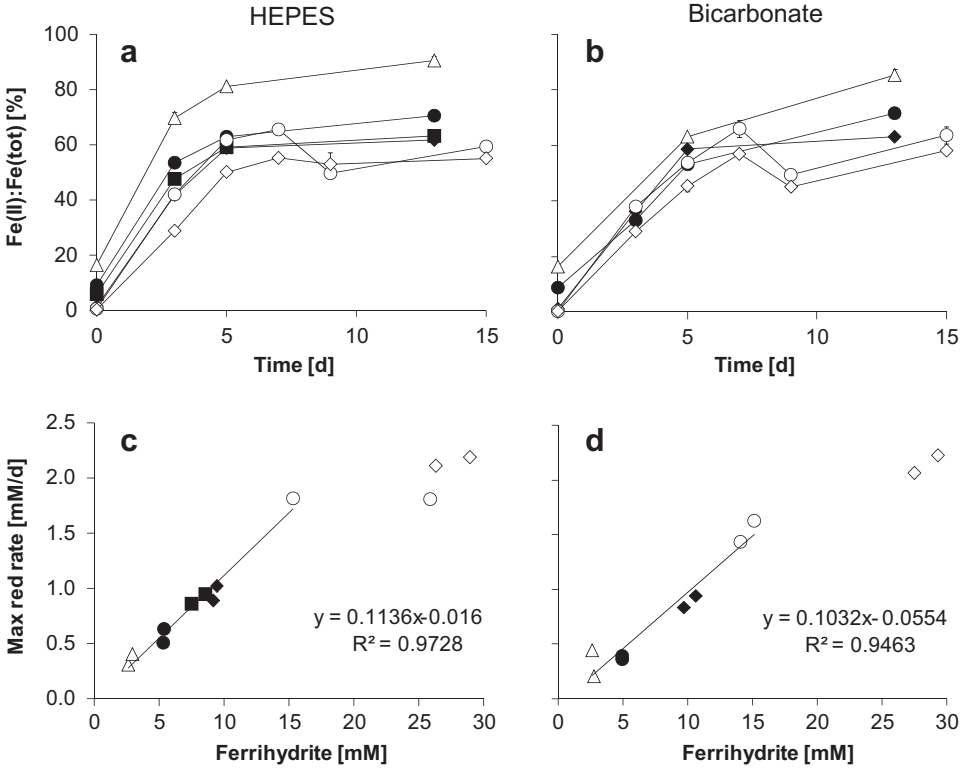

Fig. 2. Reduction of ferrihydrite by *S. oneidensis* MR-1 in (a) 12 mM HEPES and (b) 30 mM bicarbonate buffered LML medium determined by 0.5 M HCl extraction. Ferrihydrite concentrations: (Δ) 2.5 mM, (●) 5 mM, (■) 7.5 mM, (♦) 10 mM, (○) 15 mM and (◇) 30 mM. Error bars indicate range of duplicate culture bottles. Bars not visible are smaller than the symbols. (c, d) Maximum Fe(III) reduction rates (Max red rate) depending on ferrihydrite concentration in (c) 12 mM HEPES and (d) 30 mM bicarbonate buffered LML medium. Solid line represents linear correlation for data from set-ups containing ⩽15 mM ferrihydrite.

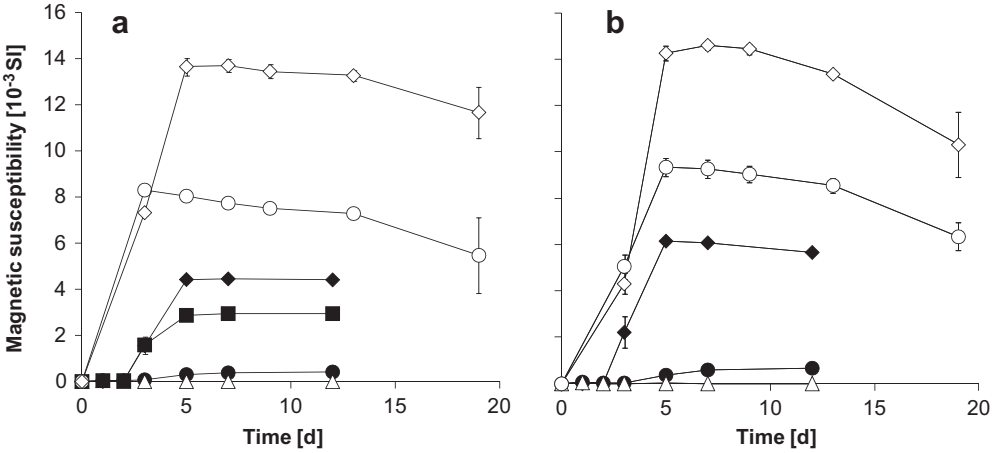

Fig. 3. Magnetic susceptibility over time in batch cultures of *S. oneidensis* MR-1 reducing ferrihydrite in (a) 12 mM HEPES and (b) 30 mM bicarbonate buffered LML medium. Ferrihydrite concentrations: (Δ) 2.5 mM, (●) 5 mM, (■) 7.5 mM, (♦) 10 mM, (○) 15 mM and (◇) 30 mM. Error bars indicate range of duplicate culture bottles. Bars not visible are smaller than the symbols.

bicarbonate versus PIPES buffer. These authors found that magnetite is formed in both buffer systems. While magnetite was the only mineral product in set-ups containing PIPES buffer, magnetite was only a minor fraction of the mineral products in bicarbonate buffered medium, with siderite being the main secondary mineral phase. However, as Fredrickson et al. (1998) identified their mineral products only after 20 days of incubation, it cannot be ruled out that in earlier stages of their experiments magnetite was dominant even in bicarbonate buffered medium followed by further reduction and transformation of the magnetite to siderite. This would correlate well with our observations in bicarbonate buffered medium, as we found siderite formation and a decrease in magnetite content during later stages of our FH reduction experiments (see below).

In our experiments with 15 mM and 30 mM FH in bicarbonate as well as HEPES buffered medium, after the initial rapid increase, the MS started to decrease after 9 days of incubation (Fig. 3) suggesting either further reduction and dissolution of the magnetite maybe followed by the formation of a non-ferrimagnetic mineral phase (e.g. siderite) or transformation into magnetite particles that show a lower volume specific MS. Lower MS values of magnetite could be due to a particle size increase from a super-paramagnetic (SP) to a single domain (SD) state. Super-paramagnetic particles close to the SP–SD transition exhibit spontaneous inversion of their magnetization and thus a much higher MS, whereas the MS of SD particles is significantly lower (Dunlop and Özdemir, 1997). The SP/SD threshold for magnetite is at a grain size of about 30 nm and biogenic magnetite frequently falls within the SP range (Zachara et al., 2002; Li et al., 2009). Therefore, although changes in the MS during microbial Fe(III) reduction can be correlated directly to the formation and dissolution of magnetite, the changes could also partially be due to grain size changes.

However, the decrease in MS observed in our FH reduction experiments correlated with μ-XRD measurements that showed the absence of magnetite and the presence of siderite in set-ups with bicarbonate buffer after 65 days of incubation (Fig. 4). This suggests further reduction and transformation of the initially formed biogenic magnetite as the dominating process for the decrease in MS. Reduction of magnetite by *S. oneidensis* MR-1 and *S. putrefaciens* CN32 along with siderite formation was also observed in bicarbonate buffered medium by Porsch et al. (2010) and Dong et al. (2000). In contrast, no mineral phase besides magnetite was identified in our set-ups with HEPES buffered medium (Fig. 5) although magnetite was also further reduced, indicated by the decrease in MS (Fig. 3). Obviously only dissolved Fe(II) was formed in these set-ups similar to studies by Kostka and Nealson (1995) and Dong et al. (2000) who also found indications that the microbial reduction of magnetite in the presence of PIPES buffer (Kostka and Nealson, 1995) and HEPES buffer (Dong et al., 2000) leads to the formation of dissolved Fe(II) without the formation of a secondary mineral phase.

In our study we could show that the extent and the maximum rates of Fe(III) reduction as well as the changes of MS over time were similar for microbial FH reduction by *S. oneidensis* MR-1 in both bicarbonate and HEPES buffered LML medium. The main difference between the two systems was the end product of FH reduction: siderite was formed in bicarbonate buffered medium whereas no additional mineral phase was formed in HEPES buffered medium. The formation of siderite ($FeCO_3$) requires bicarbonate, which was present in the bicarbonate buffered medium at a concentration of 30 mM, whereas in HEPES buffered medium 2.5 and 3.75 mM $HCO_3^-/CO_3^{2-}/CO_2$ are expected to form from lactate oxidation to acetate during reduction of 60% of 15 mM Fe(tot) and 50% of 30 mM Fe(tot), respectively. Even though precipitation of siderite is expected at these bicarbonate concentrations based on the solubility product of $\log(K) = -10.43$ (Jensen et al., 2002), siderite formation in the HEPES buffered set-ups apparently was kinetically hindered or the amounts of siderite formed were too small to be detected by μ-XRD (Fig. 5). Siderite formation in the bicarbonate system was the only significant difference between the two buffer systems. From this we conclude that the buffer system does

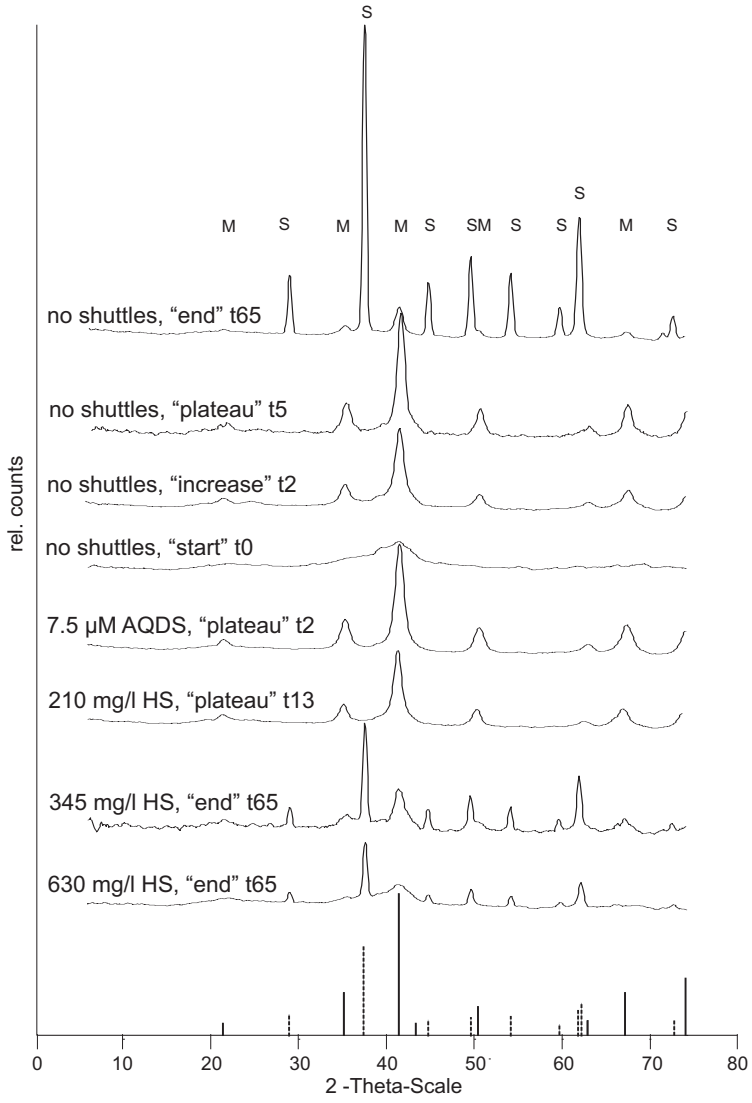

Fig. 4. X-ray diffractograms of the minerals present at different time-points during reduction of 15 mM ferrihydrite by *S. oneidensis* MR-1 in bicarbonate buffered LML medium in the presence of AQDS or humic substances (HS) or in the absence of electron shuttles. The minerals were harvested at different time-points t (given in days) at the beginning of the experiment (“start”), during (“increase”) or after (“plateau”) the increase of the magnetic susceptibility or at the end of the experiment (“end”) (see Fig. 6a). Black lines at the bottom of the figure indicate magnetite reference, dashed lines indicate siderite reference. Peaks marked M and S indicate magnetite and siderite in the samples, respectively. Diffractograms have been normalized to the same height of background signal.

not influence the microbial FH reduction, magnetite formation, and magnetite transformation per se, but rather the final product formation (upon complete Fe(III) reduction including magnetite reduction).

3.1.2. Influence of ferrihydrite concentration

Experiments were set up at FH concentrations ranging from 2.5 to 30 mM and microbial reduction of Fe(III) took place at all FH concentrations and in both media tested. The maximum Fe(III) reduction rate was linearly correlated to the initial FH concentration up to 15 mM (Fig. 2). When increasing the FH concentrations to values above 15 mM, Fe(III) reduction rates did not increase linearly anymore, suggesting that at this high FH concentration not the amount of FH present but rather other factors such as the cell number (and metabolic rate per cell) were controlling the reduction rates (see below).

Our results showed that in the presence of excess microbial cells the available mineral surface area was the limiting factor for microbial Fe(III) reduction in our experiments. The iron mineral surface area has also been identified as the factor controlling Fe(III) reduction rates by Roden and Zachara (1996) and Roden (2003). Although other factors such as the crystallinity, solubility and thus the bioavailability of the minerals also affect the Fe(III) reduction rates (Bonneville et al., 2004; Cutting et al., 2009; Bosch et al., 2010) this is only relevant when comparing different iron mineral phases present. Bonneville et al. (2006) compared reduction of the same Fe(III) mineral phase (nanohematite) at different mineral concentrations.

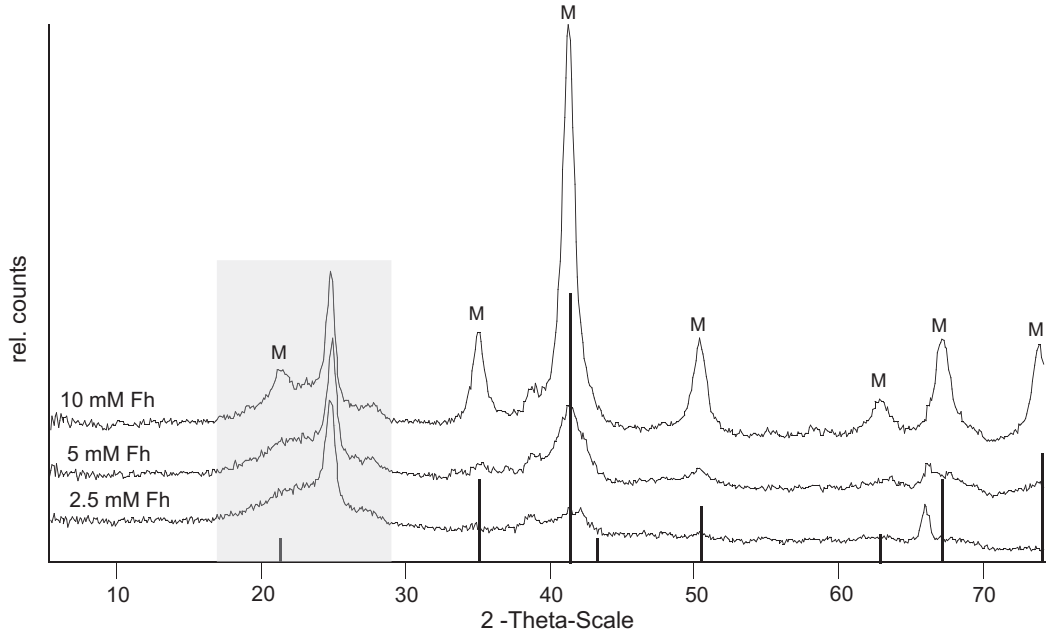

Fig. 5. X-ray diffractograms of minerals formed during ferrihydrite (FH) reduction by *S. oneidensis* MR-1 in 12 mM HEPES buffered LML medium after incubation for 20 days. FH concentrations of 2.5, 5 and 10 mM were used. Black lines at the bottom of the figure indicate magnetite reference. Peaks marked M indicate magnetite in the samples. Gray shaded area indicates signal of foil that was used to cover the minerals during measurement to prevent oxidation.

Also in their experiments, the reduction rates increased with increasing Fe(III) concentrations, but only up to a certain concentration of Fe(III). Similarly, the maximum reduction rates in our experiments leveled off at 30 mM initial FH, suggesting that the mineral surface area was limiting only below this concentration. Above this threshold, the FH was probably present in excess compared to the cell number so that all bacteria could attach directly to the FH surface leaving unoccupied mineral surface area and only an increase in cell number would lead to a further increase in maximum reduction rate (per g Fe). Additionally, aggregation of FH particles at high FH concentrations could have led to a lower accessible FH surface and thereby could have influenced the reduction rates. Overall, the absence of a further increase of reduction rates at 30 mM FH suggests that factors other than the available mineral surface area, in particular the metabolic activity, i.e. the substrate turnover over time and therefore the cell number, started to control the Fe(III) reduction rate. A transition from surface area limitation to cell limitation in microbial Fe(III) mineral reduction experiments with increasing mineral concentrations was also described by Roden and Zachara (1996).

In order to study the effect of different total FH concentrations on microbial magnetite formation, the MS was followed over time (Fig. 3). While no magnetite was formed in set-ups with 2.5 mM FH (Figs. 3 and 5), the MS increased over time in all set-ups with FH concentrations >2.5 mM which was due to the formation of magnetite as shown by μ-XRD measurements (Figs. 4 and 5). In both, HEPES and bicarbonate buffered medium, the magnetite formation strongly depended on the initial FH concentration. The more FH was present in the system, the higher the maximum MS measured meaning more magnetite was formed regardless of the buffer system used. In set-ups containing 5 mM FH the MS increased only to ca. 0.5×10^{-3} SI, while the MS in set-ups containing 30 mM FH reached maximum values of ca. 14×10^{-3} SI (Fig. 3). However, the initial FH concentration not only affected the amount of magnetite formed, but also its crystallinity as can be seen in Fig. 5 for set-ups with 12 mM HEPES buffered medium. At an initial FH concentration of 10 mM, prominent and sharp magnetite reflections were observed in the diffractogram. At initial FH concentrations of 5 mM, the signals were much broader and smaller indicating lower crystallinity (caused e.g. by more defects in the crystal lattice such as inclusions or vacancies) of the formed mineral products (Spieß et al., 2009). At initial FH concentrations of 2.5 mM no signals for magnetite were present in the μ-XRD data.

These findings indicate that the total iron concentration (in form of FH) in the system is an important factor controlling if, and to which extent, magnetite formation takes place. Such a behavior has been suggested before by Bazylinski et al. (2007), but was not systematically studied. Most experimental studies in which magnetite formation during microbial FH reduction was observed were conducted at higher FH concentrations (20–200 mM) (Lovley et al., 1987; Fredrickson et al., 1998; Zachara et al., 2002; Coker et al., 2008). Thus, these studies can be compared to our set-ups with higher FH concentrations, where magnetite formation was observed, but not to the set-ups with 2.5 mM FH, which lacked magnetite formation. One exception is the work by Perez-Gonzalez et al. (2010), who found magnetite formation during reduction of ca. 2 mM FH by *S. oneidensis* ATCC 700550. The different observations made in our experiments compared with the work of Perez-Gonzalez et al. (2010) might be due to differences in

the volume of the batch cultures (750 and 70 mL of medium in the experiments by Perez-Gonzalez et al. (2010) compared to 25 mL in our experiments). Although the concentration per volume was also 2 mM, due to rapid sedimentation of the heavy FH particles (density 3.8 g/cm^3 (Schwertmann and Cornell, 2000)), the thickness of the layer of FH at the bottom of the incubation vial (70 mL) is probably comparable to a set-up with 5–6 mM FH in 25 mL volume. Therefore, in the experiments by Perez-Gonzalez et al. (2010) the FH concentrations probably were locally similar to our 5 mM FH set-ups leading to magnetite formation.

In addition to the total amount of FH present, the Fe(II) concentration built up during FH reduction is the second important factor in controlling microbial magnetite formation, as it has been reported by Zachara et al. (2002). These authors found that magnetite was formed in FH reduction experiments only at certain Fe(II) formation rates (i.e. reduction rates). If Fe(II) concentrations at the FH surface were too low due to lower reduction rates, the FH transformed into goethite. On the other hand, at very high dissolved Fe(II) concentrations (i.e. very high reduction rates) the biomineralization process was dominated by the interaction of dissolved Fe(II) with bicarbonate forming siderite (Zachara et al., 2002). In order to analyze in more detail the influence of the Fe(II) concentration on the initiation of magnetite formation in our systems, the Fe(II) concentration at the time point when the MS started to increase (time point "Lower

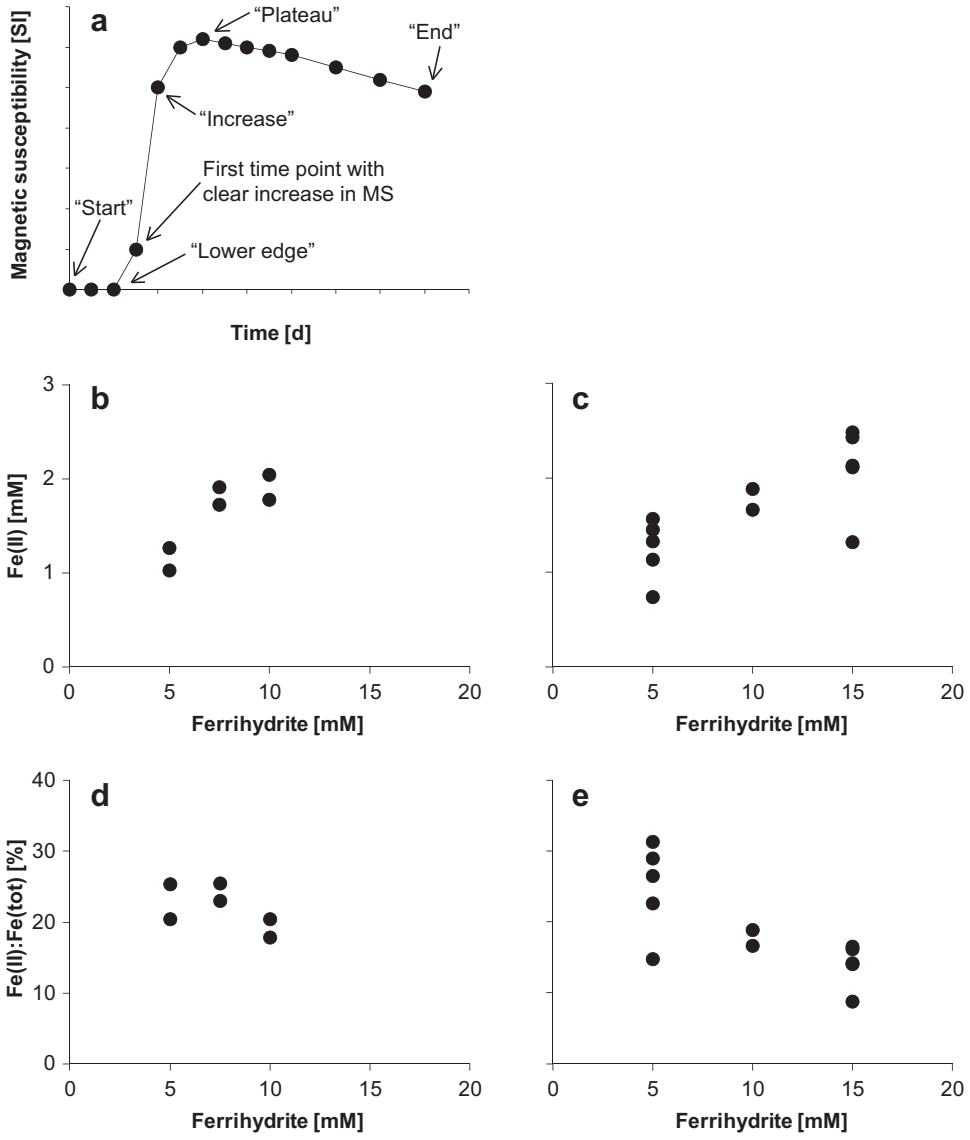

Fig. 6. Reduction of ferrihydrite by *S. oneidensis* MR-1. (a) Typical development of MS with indication of the time point "Lower edge" at which Fe(II) concentration and Fe(II):Fe(tot) ratio were investigated and time points "Start", "Increase", "Plateau" and "End" at which μ-XRD was measured (Fig. 4). (b, c) Fe(II) extractable with 0.5 M HCl at time point "Lower edge" for (b) HEPES buffered and (c) bicarbonate buffered LML medium. (d, e) Corresponding Fe(II):Fe(tot) ratios for (d) HEPES and (e) bicarbonate buffered LML medium. Each data point in (b–c) represents an individual culture bottle. At each ferrihydrite concentration several individual bottles have been set up. (d–e) shows Fe(II)/Fe(tot) data for the same bottles as shown in (b–c).

edge", see Fig. 6a) was plotted against the initial FH concentration (Fig. 6). We found that with increasing FH concentrations increasing Fe(II) concentrations were also necessary to initiate magnetite formation (Fig. 6b and c).

Magnetite formation has been described during the reduction of hematite (Behrends and Van Cappellen, 2007), lepidocrocite (O'Loughlin et al., 2010) as well as during the reduction of poorly crystalline iron phases like FH (Fredrickson et al., 1998; Bazylinski et al., 2007). While it has been suggested that magnetite is formed during hematite reduction by dissolution–reprecipitation mechanisms (Behrends and Van Cappellen, 2007), the magnetite formation mechanism during FH reduction is controversial. Bazylinski et al. (2007) proposed a solid-state conversion of FH to magnetite, whereas Cornell and Schwertmann (2003) claimed that FH is dissolved and reprecipitated as magnetite and Tronc et al. (1992) even suggested a combination of both mechanisms. In any case, it is generally accepted that magnetite formation from FH requires the interaction between dissolved Fe(II) and FH (Tronc et al., 1992; Zachara et al., 2002; Yang et al., 2010). The fact that the beginning of magnetite formation (that means the point when the first ferrihydrite is converted into magnetite), indicated by a sharp increase in MS, in our set-ups with different FH concentrations depended on the Fe(II) concentration present, suggests that a certain threshold concentration of Fe(II) adsorbed at the FH surface is necessary for the start of the formation of magnetite. If this is the case, the necessary Fe(II) concentration for initiating magnetite formation should be linearly correlated to the total iron concentration in the system and magnetite formation should start at the same Fe(II):Fe(tot) ratio for set-ups with different initial FH concentrations. However, we found that the Fe(II):Fe(tot) ratio at the starting point of magnetite formation was not the same for the different initial FH concentrations, but slightly decreased with increasing initial FH concentration (Fig. 6). This means that with increasing initial FH concentration, the amount of Fe(II) necessary to initiate magnetite formation decreased. Sorption of Fe(II) to the FH surface probably increased until a certain local threshold value of Fe(II) per nm^2 surface was reached to initiate magnetite formation. As we have recently observed that with increasing FH concentration, aggregation of the FH particles occurs (Amstaetter, 2009), we hypothesize that this aggregation leads to a lower relative surface area available for Fe(II) sorption and therefore lower Fe(II) concentrations are sufficient to reach the local Fe(II):Fe(tot) ratio necessary to initiate magnetite formation. Indeed, the rate and extent of aggregation of Fe(0) mineral particles has been found to increase with increasing iron mineral concentration (Phenrat et al., 2007). Cwiertny et al. (2008) and Nurmi et al. (2005) described that aggregation of goethite and Fe(0) particles, respectively, reduces the effective mineral surface area and thus the number of available surface sites.

3.2. Magnetite formation and transformation during ferrihydrite reduction: influence of humic substances/electron shuttles

HS are known to stimulate microbial Fe(III) reduction by shuttling electrons between microbial cells and poorly soluble Fe(III) minerals (Lovley et al., 1996). In addition to this electron shuttling effect, at pH-neutral conditions, the negatively charged HS have a strong affinity to the positively charged Fe(III) mineral surface and show strong sorption (Kaiser et al., 2007) (Fig. 1). However, little is known about the effect of the presence of HS on microbial magnetite formation, either via electron shuttling or by sorption to the mineral surfaces. Therefore, we performed FH reduction experiments with *S. oneidensis* MR-1 in bicarbonate buffered LML medium to examine the effect of different HS concentrations (210–630 mg/L) on the reduction of 15 mM FH. Set-ups amended with 7.5 and 23.4 μM AQDS were used as control experiments for the presence of electron shuttles that sorb only to a very low extent to FH (Wolf et al., 2009).

Although HS were described to stimulate microbial reduction of Fe(III) minerals, in set-ups containing 15 mM FH and 210–630 mg/L total HS, FH reduction took place to a lower extent and with a slightly reduced rate compared to HS free set-ups (Fig. 7). However, we observed differences between the different HS concentrations: The lowest maximum reduction rates (measured from two parallel culture bottles) were obtained in the presence of 210–345 mg/L total HS (0.83 ± 0.01 and 0.72 ± 0.03 mM Fe/d, respectively). In the presence of 630 mg/L HS the maximum reduction rates were slightly higher (1.29 ± 0.00 mM Fe/d) than in the presence of lower HS concentrations, however not as high as in set-ups without HS (1.69 ± 0.04 mM Fe/d). These differences in maximum reduction rates observed indicate that different concentrations of HS had different influences on microbial FH reduction.

Besides shuttling electrons between cells and Fe(III) minerals, (e.g. Lovley et al., 1996; Jiang and Kappler, 2008), HS are expected to affect microbial iron reduction by sorption to the iron minerals. We found that at HS concentrations below 200 mg HS/g FH (corresponding to 320 mg HS/L for 15 mM FH present in our reduction experiments) virtually all HS in the system were sorbed to the FH (Fig. 8). This suggests that in our 15 mM FH set-ups containing 210 mg/L and 345 mg/L total HS (corresponding to 131 and 215 mg HS/g FH, respectively) the HS were sorbed more or less completely to the FH. Therefore, stimulation of Fe(III) reduction by electron shuttling was not possible in these set-ups since HS electron shuttling requires a minimum concentration of dissolved HS of 5–10 mg C/L (Jiang and Kappler, 2008). Additionally, the reduced maximum reduction rates observed in the presence of 210 mg/L and 345 mg/L total HS in comparison to HS-free set-ups even suggest that sorption of HS actually decreases Fe(III) reduction rates by reducing the bioavailable mineral surface area either by blocking bioaccessible surface sites or by formation of FH–HS aggregates that are less accessible (have a lower surface area per g FH) than non-HS-coated FH. Most previous studies on HS electron shuttling have been conducted at significantly higher HS concentrations than were used in the present work (e.g. 3118 mg HS/g FH in the work of Lovley et al. (1996)) and the fraction of HS sorbed compared to the dissolved fraction was not quantified. Therefore, the effects of HS sorption on the Fe(III) reduction rates observed in our study have not been

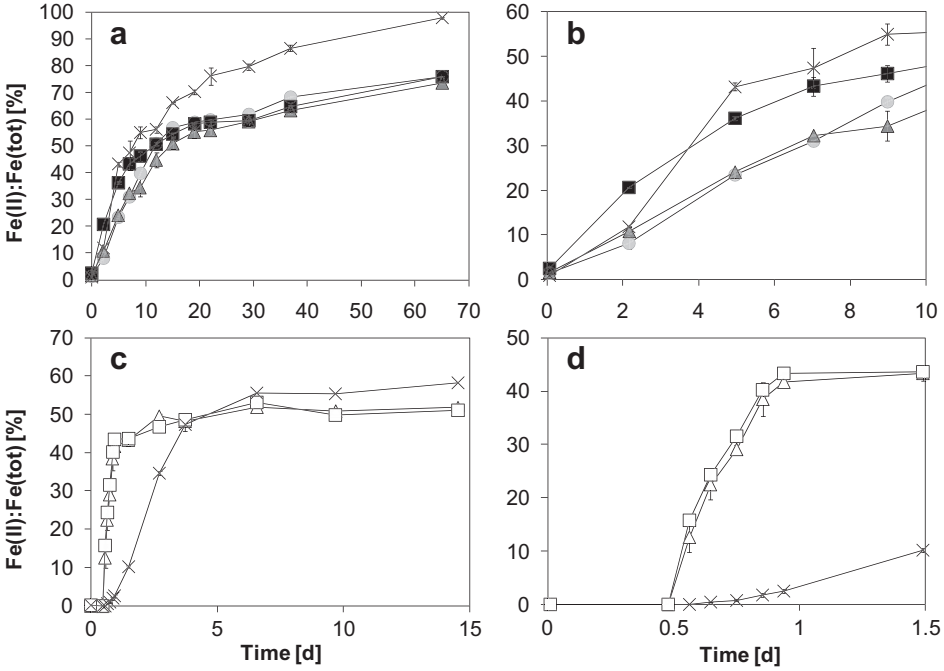

Fig. 7. Reduction of 15 mM ferrihydrite by *S. oneidensis* MR-1 in bicarbonate buffered LML medium in the presence of different electron shuttles. (a) set-ups amended with humic substances (HS), 65 days of incubation, (b) detailed view of the first 10 days of a, (c) set-ups amended with AQDS, 15 days of incubation, (d) detailed view of the first 1.5 days of c. (X) no shuttles, (●) 210 mg/L HS, (▲) 345 mg/L HS, (■) 630 mg/L HS, (Δ) 7.5 μM AQDS, (□) 23.4 μM AQDS. Error bars indicate the range of duplicate culture bottles. Bars not visible are smaller than the symbol. Note the different scales of the axes.

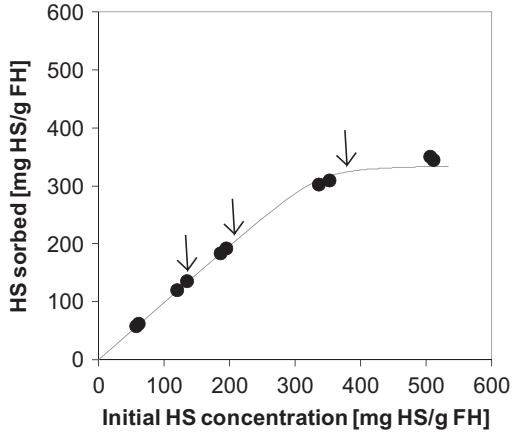

Fig. 8. Sorption of humic substances (HS) to 15 mM (1.6 g/L) ferrihydrite (FH) in the presence of bicarbonate buffered LML medium. Gray line: Langmuir sorption isotherm ($K = 0.43$, $n = 337.7$ mg HS/g FH) modeled by minimizing the error. Arrows indicate concentrations used in this study.

discussed systematically in the literature so far. One exception is the study by O'Loughlin et al. (2010), who described that the addition of HS to microbial lepidocrocite reduction experiments led to reduced reduction rates, probably due to HS sorption to the mineral surface. As discussed in Section 3.1.2, in our experiments, the microbial reduction of 15 mM FH at the cell numbers present seemed to be limited by the iron mineral surface area. Therefore, a further decrease of the available surface area due to HS sorption to FH is expected to lead to a lower Fe(III) reduction rate in set-ups with 210 and 345 mg/L total HS.

In contrast, the scenario was different in the presence of 630 mg/L total HS (393 mg HS/g FH), since sorbed as well as dissolved HS were present in these set-ups (Fig. 8). Therefore, in set-ups with 630 mg/L total HS, electron shuttling by HS could take place leading to an increase in maximum reduction rates compared to the set-ups with sorbed HS only. In positive controls for electron shuttling, the model quinone AQDS was used. This quinone compound has been demonstrated to function as an efficient electron shuttle between bacterial cells like *S. oneidensis* MR-1 and Fe(III) minerals (Lovley et al., 1998; Lies et al., 2005), but shows only very little sorption to iron minerals (Wolf et al., 2009). The set-ups with AQDS (Fig. 7) showed that the presence of this electron shuttle, which does not sorb (or only to a very low extent) to the FH, increased the maximum reduction rates from 3.0 ± 0.1 mM Fe/d in the absence of electron shuttles to 22.7 ± 4.9 mM Fe/d and 28.4 ± 0.4 mM Fe/d in the presence of 7.5 and 23.4 μM AQDS, respectively. This indicates a strong effect of electron shuttling on the Fe(III) reduction rate at the FH and cell concentrations used in our experiments. Therefore, the increased Fe(III) reduction rates observed in the presence of 630 mg/L total HS compared to set-ups containing 210 and 345 mg/L total HS (Fig. 7a and b) were most likely due to the effect of electron shuttling by dissolved HS (Lovley et al., 1996). However, a significant fraction of the 630 mg/L total HS (corresponding to 393 mg total HS/g FH) was still sorbed to the FH (Fig. 8). Since the

maximum reduction rates in these set-ups were still lower than the reduction rates in set-ups without HS, the sorbed fraction of HS obviously still had an inhibiting effect on the reduction rate. Thus, in the presence of 630 mg/L total HS, the two effects of HS sorption (inhibiting Fe(III) reduction) and HS electron shuttling (stimulating Fe(III) reduction) were cancelling out each other leading to an overall intermediate reduction rate. This illustrates that even though electron shuttling by dissolved HS took place in this case of low concentration of dissolved HS, it was not strong enough to completely overcome the surface area limitation caused by the sorbed HS.

In addition to external electron shuttles such as AQDS and HS, Marsili et al. (2008) and von Canstein et al. (2008) described that *S. oneidensis* MR-1 is able to produce and excrete flavins which can also function as electron shuttles between bacterial cells and Fe(III) minerals. Since the secretion of these redox mediators seems to be more or less independent of the geochemical conditions (Von Canstein et al., 2008), MR-1 can be expected to excrete the same amount of redox mediators in all of the different set-ups used in our experiments. Nevertheless, a stimulating effect of AQDS and an inhibiting effect of sorbed HS on the Fe(III) reduction rates was observed in our study. This could be due to the fact that the concentrations of flavins detected in the experiments by Marsili et al. (2008) and von Canstein et al. (2008) (0.1–0.6 μM) were significantly lower than the lowest concentrations of electron shuttles used in our experiments (7.5 μM AQDS). Thus, the amount of endogenous electron shuttles excreted by MR-1 could simply be too low to completely overcome the surface area limitation in our systems. This confirms previous findings of Jiang and Kappler (2008), who described that the stimulating effect of electron shuttles on microbial Fe(III) reduction depends on the concentration of the electron shuttles.

Besides Fe(III) reduction rates we also followed the MS during 15 mM FH reduction by MR-1 in the presence of HS compared to experiments in the absence of HS. Highest MS values ($9.691 \pm 0.12 \times 10^{-3}$ and $9.446 \pm 0.081 \times 10^{-3}$ SI, respectively) and the steepest increase in MS ($3.276 \pm 0.194 \times 10^{-3}$ and $3.763 \pm 0.398 \times 10^{-3}$ SI/d, respectively) were measured in treatments without HS and in treatments with 210 mg/L total HS (Fig. 9). With increasing HS concentrations, the maximum MS value as well as the slope of the MS curve decreased indicating that the extent as well as the maximum rate of magnetite formation decreased. In the presence of 630 mg/L total HS almost no magnetite formation took place as shown by MS measurements (Fig. 9) and by μ-XRD measurements (Fig. 4). In treatments without HS, the MS decreased again significantly after reaching its maximum value (Fig. 9) while Fe(II) still increased (Fig. 7) indicating magnetite reduction. However, in treatments with 210 and 345 mg/L total HS, the MS decreased only slightly within 65 days of incubation (Fig. 9a). Thus, in the presence of HS, the further reduction of magnetite and subsequent formation of siderite, which was responsible

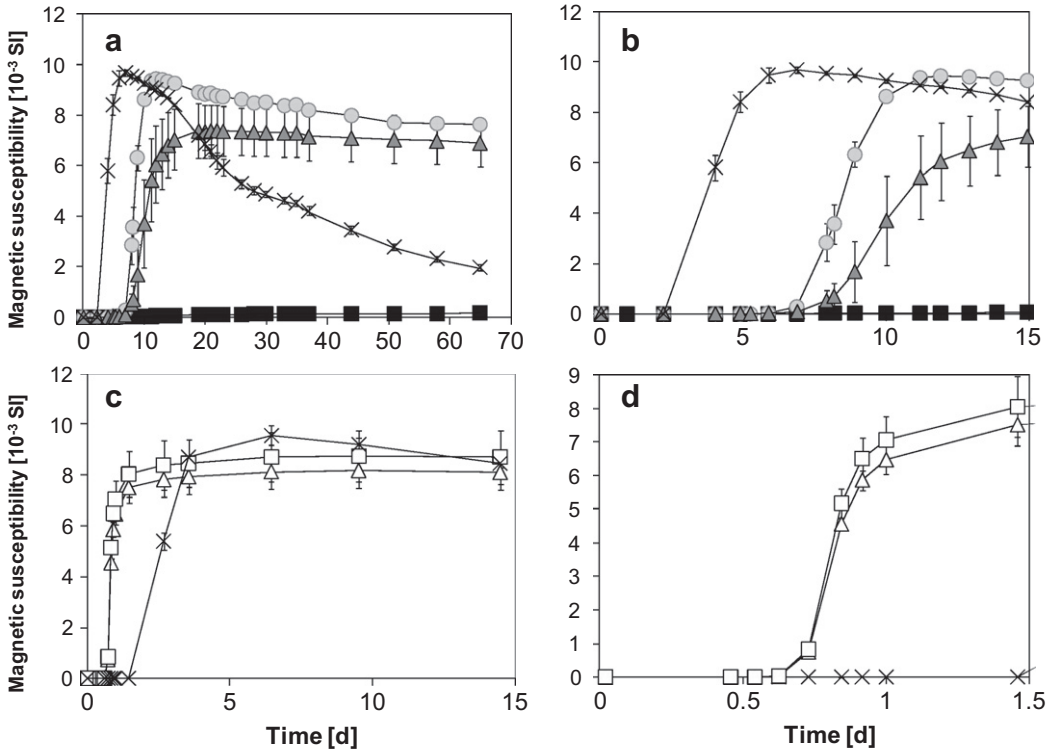

Fig. 9. Magnetic susceptibility during reduction of 15 mM ferrihydrite by *S. oneidensis* MR-1 in the presence of different electron shuttles. (a) set-ups amended with humic substances (HS), 65 days of incubation, (b) detailed view of the first 15 days of a, (c) set-ups amended with AQDS, 15 days of incubation, (d) detailed view of the first 1.5 days of c. (X) no electron shuttles, (●) 210 mg/L HS, (▲) 345 mg/L HS, (■) 630 mg/L HS, (Δ) 7.5 μM AQDS, (□) 23.4 μM AQDS. Error bars indicate the range of duplicate culture bottles. Bars not visible are smaller as the symbol. Note the different scales of the axes.

for the decrease in MS in HS-free bicarbonate buffered set-ups (Section 3.1.1), seemed to be slowed down considerably. In contrast, the set-ups with AQDS showed only in the first 15 days stable MS values (Fig. 9c) and then a further decrease in MS (data not shown) similar to the set-ups without electron shuttles suggesting further reduction of the magnetite also in the set-ups with AQDS.

As discussed before, there are several possible effects of HS on microbial Fe(III) reduction and magnetite formation, e.g. sorption of HS to iron minerals, HS electron shuttling between microorganisms and Fe(III) minerals or complexation of Fe(II) by HS (Fig. 1). The set-ups with AQDS illustrate the effect of electron shuttling on microbial magnetite formation. The presence of AQDS did not inhibit magnetite formation (Fig. 9c and d). On the contrary, the MS increased even faster in the presence of 7.5 and 23.4 μM AQDS than in the absence of AQDS. This indicates that the inhibiting effect on the magnetite formation rates measured in the presence of higher HS concentrations cannot be due to the effect of electron shuttling, but rather due to Fe(II) complexation by HS or due to HS sorption to the FH. The amount of Fe(II) that can be complexed by the amount of HS present in the system can be estimated to 1.54, 2.53, and 4.62 mM Fe(II) in set-ups with 210, 345, and 630 mg/L HS, respectively (based on Amstaetter (2009)). As this corresponds to 41.6, 68.9 and >100% of the Fe(II) present at the time-point before magnetite formation starts, complexation by HS could lead to a considerable reduction of the amount of dissolved Fe(II) available for the interaction with the FH and, thus, to a decrease in magnetite formation. Alternatively, HS sorption to the FH could be responsible for the reduced or absent magnetite formation in the presence of HS. The amount of sorbed HS increased from set-ups with 210 mg/L total HS (131 mg total HS/g FH) and set-ups with 345 mg/L total HS (215 mg total HS/g FH) to set-ups with 630 mg/L total HS (393 mg total HS/g FH) (Fig. 8). As there was the same amount of FH present in all set-ups (15 mM), the increased amount of sorbed HS means that there was less free surface area available at higher HS concentrations. As discussed in Section 3.1.2, magnetite formation depends on the interaction of Fe(II) with the FH, which requires sorption of dissolved Fe(II) to the FH surface. Therefore, as the mineral surface area available for Fe^{2+} sorption decreased with increasing HS concentration (due to HS sorption) the magnetite formation rate decreased likewise. In the presence of 210 mg/L total HS only about 30% of the FH surface were covered with sorbed HS (estimated from Fig. 8 based on monolayer coverage of HS on the FH surface) which seems to be too low to significantly inhibit Fe^{2+} interaction with the FH. Therefore, the rate and extent of magnetite formation measured in these set-ups was in the same order of magnitude as the magnetite formation rate measured in the absence of HS. In the presence of 345 mg/L total HS, on the other hand, the maximum magnetite formation rate was considerably lower compared to magnetite formation rates measured in the absence of HS indicating that at an estimated coverage of ca. 50% of the surface area (Fig. 8) enough of the surface binding sites for Fe^{2+} were blocked by sorbed HS to limit the interaction between Fe^{2+} and FH necessary to initiate rapid magnetite formation. At the highest HS concentration of 630 mg/L magnetite formation did not take place at all, even though FH was reduced and dissolved Fe(II) was present. This suggests that magnetite formation was prevented by an almost complete blocking of Fe^{2+} binding sites by HS as supported by the HS sorption isotherm (Fig. 8). Additionally, the sorbed HS could also interfere with the recrystallization of FH to magnetite by interrupting the structure of the mineral lattice, similar to the effect of exopolysaccharides on the crystallinity observed during the precipitation of ferrihydrite (Mikutta et al., 2008). These findings are in agreement with experiments reported by Jones et al. (2009) and O'Loughlin et al. (2010). Jones et al. (2009) found that the Fe(II)-catalyzed recrystallization of 2.5 mM FH reacting with a solution of 1 mM $FeSO_4$ in abiotic experiments at neutral pH was prevented by adsorption of 150 mg/L HS (561.3 mg HS/g FH) to the iron mineral surface. They also suggested that sorbed HS prevented the adsorption of Fe^{2+} to the mineral surface and thus the interaction of Fe^{2+} with FH, which was essential for the recrystallization process.

3.3. Implications for magnetite formation in the environment

Magnetite is one of the most important mineral products of microbial Fe(III) reduction. In addition to the importance of microbial formation and dissolution of iron minerals in controlling the fate of pollutants in the environment, magnetite formation is of special interest due to its magnetic properties, which make it one of the most important factors determining magnetic soil properties. The results of the present study highlight the importance of the interaction of dissolved Fe(II) with FH for the formation of magnetite. Different mechanisms of magnetite formation are discussed in the literature: solid-state conversion of FH (Bazylinski et al., 2007), dissolution of the FH and subsequent reprecipitation of magnetite (Cornell and Schwertmann, 2003) or a combination of both (Tronc et al., 1992). In spite of the differences in the proposed mechanisms, all authors agree on the importance of the presence of Fe^{2+} for magnetite formation. Thus, it is expected that processes that constrain the interaction of FH with dissolved Fe(II) will reduce the rates and/or extent of magnetite formation. Based on the results of the present study, such processes could be either HS sorption to the FH surface blocking the available surface sites for Fe^{2+} adsorption, complexation of Fe(II) by HS or the formation of an unfavorable Fe(II):Fe(III) ratio (either too high or too low) leading to an unfavorable degree of FH surface saturation with Fe^{2+}.

Our results suggest that magnetite formation in natural environments strongly depends on the geochemical parameters present, in particular on the presence of dissolved HS. In soils of low iron content, magnetite formation could be limited by low iron concentration or inhibited by adsorption of HS to the Fe(III) mineral surface. In contrast, in soils of higher iron content with the simultaneous presence of low concentrations of dissolved HS that can sorb to the mineral surface, microbial Fe(III) reduction is more likely leading to considerable magnetite formation.

Our results also suggest that in order to better understand microbial Fe(III) reduction and magnetite formation

in the environment, in laboratory experiments more attention has to be paid to the geochemical parameters present in the environment. In particular the use of model quinones such as AQDS instead of redox-active HS might produce misleading results, as our study showed significant differences regarding Fe(III) reduction and magnetite formation between parallel treatments with AQDS and HS.

ACKNOWLEDGEMENTS

We would like to thank Christoph Berthold, Katja Amstaetter and Inga Köhler for μ-XRD measurements, Katja Amstaetter for protein content measurements, Moti Lal Rijal for support with MS measurements and Massimo Rolle for help with modeling the Langmuir sorption isotherm. This study was funded by the research group FOR 580 of the German Research Foundation (DFG) "Electron Transfer Processes in Anoxic Aquifers".

REFERENCES

Amstaetter K. (2009) Microbial iron reduction influenced by humic acids and redox transformation of arsenic by reactive iron minerals. Ph. D. thesis, Eberhard Karls Universität, Tübingen.

Amstaetter K., Borch T., Larese-Casanova P. and Kappler A. (2010) Redox transformation of arsenic by Fe(II)-activated goethite (alpha-FeOOH). *Environ. Sci. Technol.* **44**, 102–108.

Bauer I. and Kappler A. (2009) Rates and extent of reduction of Fe(III) compounds and O-2 by humic substances. *Environ. Sci. Technol.* **43**, 4902–4908.

Bazylinski D. A., Frankel R. B. and Konhauser K. O. (2007) Modes of biomineralization of magnetite by microbes. *Geomicrobiol. J.* **24**, 465–475.

Behrends T. and Van Cappellen P. (2007) Transformation of hematite into magnetite during dissimilatory iron reduction – conditions and mechanisms. *Geomicrobiol. J.* **24**, 403–416.

Bell P. E., Mills A. L. and Herman J. S. (1987) Biogeochemical conditions favoring magnetite formation during anaerobic iron reduction. *Appl. Environ. Microbiol.* **53**, 2610–2616.

Benz M., Schink B. and Brune A. (1998) Humic acid reduction by *Propionibacterium freudenreichii* and other fermenting bacteria. *Appl. Environ. Microbiol.* **64**, 4507–4512.

Bonneville S., Van Cappellen P. and Behrends T. (2004) Microbial reduction of iron(III) oxyhydroxides: effects of mineral solubility and availability. *Chem. Geol.* **212**, 255–268.

Bonneville S., Behrends T., Van Cappellen P., Hyacinthe C. and Roling W. F. M. (2006) Reduction of Fe(III) colloids by *Shewanella putrefaciens*: a kinetic model. *Geochim. Cosmochim. Acta* **70**, 5842–5854.

Bosch J., Heister K., Hofmann T. and Meckenstock R. U. (2010) Nanosized iron oxide colloids strongly enhance microbial iron reduction. *Appl. Environ. Microbiol.* **76**, 184–189.

Cervantes F. J., de Bok F. A. M., Tuan D. D., Stams A. J. M., Lettinga G. and Field J. A. (2002) Reduction of humic substances by halorespiring, sulphate-reducing and methanogenic microorganisms. *Environ. Microbiol.* **4**, 51–57.

Coates J. D., Ellis D. J., Blunt-Harris E. L., Gaw C. V., Roden E. E. and Lovley D. R. (1998) Recovery of humic-reducing bacteria from a diversity of environments. *Appl. Environ. Microbiol.* **64**, 1504–1509.

Coker V. S., Bell A. M. T., Pearce C. I., Pattrick R. A. D., van der Laan G. and Lloyd J. R. (2008) Time-resolved synchrotron powder X-ray diffraction study of magnetite formation by the Fe(III)-reducing bacterium *Geobacter sulfurreducens*. *Am. Mineral.* **93**, 540–547.

Cornell R. M. and Schwertmann U. (2003) *The iron oxides: structure*. Wiley-VCH, Weinheim.

Cutting R. S., Coker V. S., Fellowes J. W., Lloyd J. R. and Vaughan D. J. (2009) Mineralogical and morphological constraints on the reduction of Fe(III) minerals by *Geobacter sulfurreducens*. *Geochim. Cosmochim. Acta* **73**, 4004–4022.

Cwiertny D. M., Handler R. M., Schaefer M. V., Grassian V. H. and Scherer M. M. (2008) Interpreting nanoscale size-effects in aggregated Fe-oxide suspensions: reaction of Fe(II) with goethite. *Geochim. Cosmochim. Acta* **72**, 1365–1380.

Dong H. L., Fredrickson J. K., Kennedy D. W., Zachara J. M., Kukkadapu R. K. and Onstott T. C. (2000) Mineral transformation associated with the microbial reduction of magnetite. *Chem. Geol.* **169**, 299–318.

Dunlop D. J. and Özdemir Ö. (1997) *Rock magnetism: fundamentals and frontiers*. Cambridge University Press, Cambridge.

El-Naggar M. Y., Wanger G., Leung K. M., Yuzvinsky T. D., Southam G., Yang J., Lau W. M., Nealson K. H. and Gorby Y. A. (2010) Electrical transport along bacterial nanowires from *Shewanella oneidensis* MR-1. *Proc. Natl. Acad. Sci.* **107**, 18127–18131.

Fredrickson J. K., Zachara J. M., Kennedy D. W., Dong H. L., Onstott T. C., Hinman N. W. and Li S. M. (1998) Biogenic iron mineralization accompanying the dissimilatory reduction of hydrous ferric oxide by a groundwater bacterium. *Geochim. Cosmochim. Acta* **62**, 3239–3257.

Fredrickson J. K., Kota S., Kukkadapu R. K., Liu C. X. and Zachara J. M. (2003) Influence of electron donor/acceptor concentrations on hydrous ferric oxide (HFO) bioreduction. *Biodegradation* **14**, 91–103.

Hansel C. M., Benner S. G., Nico P. and Fendorf S. (2004) Structural constraints of ferric (hydr)oxides on dissimilatory iron reduction and the fate of Fe(II). *Geochim. Cosmochim. Acta* **68**, 3217–3229.

Hansel C. M., Benner S. G. and Fendorf S. (2005) Competing Fe(II)-induced mineralization pathways of ferrihydrite. *Environ. Sci. Technol.* **39**, 7147–7153.

Hegler F., Posth N. R., Jiang J. and Kappler A. (2008) Physiology of phototrophic iron(II)-oxidizing bacteria: implications for modern and ancient environments. *FEMS Microbiol. Ecol.* **66**, 250–260.

Hohmann C., Winkler E., Morin G. and Kappler A. (2010) Anaerobic Fe(II)-oxidizing bacteria show as resistance and immobilize as during Fe(III) mineral precipitation. *Environ. Sci. Technol.* **44**, 94–101.

Islam F. S., Gault A. G., Boothman C., Polya D. A., Charnock J. M., Chatterjee D. and Lloyd J. R. (2004) Role of metal-reducing bacteria in arsenic release from Bengal delta sediments. *Nature* **430**, 68–71.

Jensen D. L., Boddum J. K., Tjell J. C. and Christensen T. H. (2002) The solubility of rhodochrosite ($MnCO_3$) and siderite ($FeCO_3$) in anaerobic aquatic environments. *Appl. Geochem.* **17**, 503–511.

Jiang J. and Kappler A. (2008) Kinetics of microbial and chemical reduction of humic substances: implications for electron shuttling. *Environ. Sci. Technol.* **42**, 3563–3569.

Johnson C. M., Beard B. L., Beukes N. J., Klein C. and O'Leary J. M. (2003) Ancient geochemical cycling in the Earth as inferred from Fe isotope studies of banded iron formations from the Transvaal Craton. *Contrib. Mineral. Petrol.* **144**, 523–547.

Jones A. M., Collins R. N., Rose J. and Waite T. D. (2009) The effect of silica and natural organic matter on the Fe(II)-catalysed transformation and reactivity of Fe(III) minerals. *Geochim. Cosmochim. Acta* **73**, 4409–4422.

Kaiser K., Mikutta R. and Guggenberger G. (2007) Increased stability of organic matter sorbed to ferrihydrite and goethite on aging. *Soil Sci. Soc. Am. J.* **71**, 711–719.

Kappler A. and Straub K. L. (2005) Geomicrobiological cycling of iron. *Rev. Mineral. Geochem.* **59**, 85–108.

Kostka J. E. and Nealson K. H. (1995) Dissolution and reduction of magnetite by bacteria. *Environ. Sci. Technol.* **29**, 2535–2540.

Li Y. L., Pfiffner S. M., Dyar M. D., Vali H., Konhauser K., Cole D. R., Rondinone A. J. and Phelps T. J. (2009) Degeneration of biogenic superparamagnetic magnetite. *Geobiology* **7**, 25–34.

Lies D. P., Hernandez M. E., Kappler A., Mielke R. E., Gralnick J. A. and Newman D. K. (2005) *Shewanella oneidensis* MR-1 uses overlapping pathways for iron reduction at a distance and by direct contact under conditions relevant for biofilms. *Appl. Environ. Microbiol.* **71**, 4414–4426.

Lovley D. R. and Anderson R. T. (2000) Influence of dissimilatory metal reduction on fate of organic and metal contaminants in the subsurface. *Hydrogeol. J.* **8**, 77–88.

Lovley D. R., Stolz J. F., Nord G. L. and Phillips E. J. P. (1987) Anaerobic production of magnetite by a dissimilatory iron-reducing microorganism. *Nature* **330**, 252–254.

Lovley D. R., Woodward J. C. and Chapelle F. H. (1994) Stimulated anoxic biodegradation of aromatic-hydrocarbons using Fe(III) ligands. *Nature* **370**, 128–131.

Lovley D. R., Coates J. D., BluntHarris E. L., Phillips E. J. P. and Woodward J. C. (1996) Humic substances as electron acceptors for microbial respiration. *Nature* **382**, 445–448.

Lovley D. R., Fraga J. L., Blunt-Harris E. L., Hayes L. A., Phillips E. J. P. and Coates J. D. (1998) Humic substances as a mediator for microbially catalyzed metal reduction. *Acta Hydroch. Hydrob.* **26**, 152–157.

Maher B. A. (2009) Rain and dust: magnetic records of climate and pollution. *Elements* **5**, 229–234.

Marsili E., Baron D. B., Shikhare I. D., Coursolle D., Gralnick J. A. and Bond D. R. (2008) *Shewanella* secretes flavins that mediate extracellular electron transfer. *Proc. Natl. Acad. Sci. USA* **105**, 3968–3973.

Mikutta C., Mikutta R., Bonneville S., Wagner F., Voegelin A., Christl I. and Kretzschmar R. (2008) Synthetic coprecipitates of exopolysaccharides and ferrihydrite. Part I: characterization. *Geochim. Cosmochim. Acta* **72**, 1111–1127.

Myers C. R. and Nealson K. H. (1988) Bacterial manganese reduction and growth with manganese oxide as the sole electron-acceptor. *Science* **240**, 1319–1321.

Myers C. R. and Myers J. M. (1994) Ferric iron reduction-linked growth yields of *Shewanella-Putrefaciens* Mr-1. *J. Appl. Bacteriol.* **76**, 253–258.

Nurmi J. T., Tratnyek P. G., Sarathy V., Baer D. R., Amonette J. E., Pecher K., Wang C. M., Linehan J. C., Matson D. W., Penn R. L. and Driessen M. D. (2005) Characterization and properties of metallic iron nanoparticles: spectroscopy, electrochemistry, and kinetics. *Environ. Sci. Technol.* **39**, 1221–1230.

O'Loughlin E. J., Gorski C. A., Scherer M. M., Boyanov M. I. and Kemner K. M. (2010) Effects of oxyanions, natural organic matter, and bacterial cell numbers on the bioreduction of lepidocrocite (gamma-FeOOH) and the formation of secondary mineralization products. *Environ. Sci. Technol.* **44**, 4570–4576.

Perez-Gonzalez T., Jimenez-Lopez C., Neal A. N., Rull-Perez F., Rodriguez-Navarro A., Fernandez-Vivas A. and Ianez-Pareja E. (2010) Magnetite biomineralization induced by *Shewanella oneidensis*. *Geochim. Cosmochim. Acta* **74**, 967–979.

Phenrat T., Saleh N., Sirk K., Tilton R. D. and Lowry G. V. (2007) Aggregation and sedimentation of aqueous nanoscale zerovalent iron dispersions. *Environ. Sci. Technol.* **41**, 284–290.

Porsch K., Dippon U., Rijal M. L., Appel E. and Kappler A. (2010) In-situ magnetic susceptibility measurements as a tool to follow geomicrobiological transformation of Fe minerals. *Environ. Sci. Technol.* **44**, 3846–3852.

Raven K. P., Jain A. and Loeppert R. H. (1998) Arsenite and arsenate adsorption on ferrihydrite: kinetics, equilibrium, and adsorption envelopes. *Environ. Sci. Technol.* **32**, 344–349.

Reguera G., McCarthy K. D., Mehta T., Nicoll J. S., Tuominen M. T. and Lovley D. R. (2005) Extracellular electron transfer via microbial nanowires. *Nature* **435**, 1098–1101.

Roden E. E. (2003) Fe(III) oxide reactivity toward biological versus chemical reduction. *Environ. Sci. Technol.* **37**, 1319–1324.

Roden E. E. and Zachara J. M. (1996) Microbial reduction of crystalline iron(III) oxides: influence of oxide surface area and potential for cell growth. *Environ. Sci. Technol.* **30**, 1618–1628.

Roden E. E., Kappler A., Bauer I., Jiang J., Paul A., Stoesser R., Konishi H. and Xu H. F. (2010) Extracellular electron transfer through microbial reduction of solid-phase humic substances. *Nat. Geosci.* **3**, 417–421.

Schwertmann U. and Cornell R. M. (2000) *Iron oxides in the laboratroy: preparation and characterization*. Wiley-VCH, Weinheim.

Spieß L., Teichert G., Schwarzer R., Behnken H. and Genzel C. (2009) *Moderne röntgenbeugung: röntgendiffraktometrie für materialwissenschaftler, physiker und chemiker.*. Vieweg + Teubner, Wiesbaden.

Stevenson F. J. (1994) *Humus chemistry: genesis, composition, reactions*. John Wiley, New York.

Stookey L. L. (1970) Ferrozine – a new spectrophotometric reagent for iron. *Anal. Chem.* **42**, 779–781.

Tronc E., Belleville P., Jolivet J. P. and Livage J. (1992) Transformation of ferric hydroxide into spinel by Fe(II) adsorption. *Langmuir* **8**, 313–319.

Tufano K. J. and Fendorf S. (2008) Confounding impacts of iron reduction on arsenic retention. *Environ. Sci. Technol.* **42**, 4777–4783.

von Canstein H., Ogawa J., Shimizu S. and Lloyd J. R. (2008) Secretion of flavins by *Shewanella* species and their role in extracellular electron transfer. *Appl. Environ. Microbiol.* **74**, 615–623.

Weber K. A., Achenbach L. A. and Coates J. D. (2006) Microorganisms pumping iron: anaerobic microbial iron oxidation and reduction. *Nat. Rev. Microbiol.* **4**, 752–764.

Wolf M., Kappler A., Jiang J. and Meckenstock R. U. (2009) Effects of humic substances and quinones at low concentrations on ferrihydrite reduction by *Geobacter metallireducens*. *Environ. Sci. Technol.* **43**, 5679–5685.

Yang L., Steefel C. I., Marcus M. A. and Bargar J. R. (2010) Kinetics of Fe(II)-catalyzed transformation of 6-line ferrihydrite under anaerobic flow conditions. *Environ. Sci. Technol.* **44**, 5469–5475.

Zachara J. M., Kukkadapu R. K., Fredrickson J. K., Gorby Y. A. and Smith S. C. (2002) Biomineralization of poorly crystalline Fe(III) oxides by dissimilatory metal reducing bacteria (DMRB). *Geomicrobiol. J.* **19**, 179–207.

Associate editor: Christopher John Daughney